京都大学防災研究所年報 第 53 号 B 平成 22 年 6 月
Annuals of Disas. Prev. Res. Inst., Kyoto Univ., No. 53 B, 2010

Glacial Lake Outburst due to Moraine Dam Failure by Seepage and Overtopping with Impact of Climate Change

Badri Bhakta SHRESTHA, Hajime NAKAGAWA, Kenji KAWAIKE, Yasuyuki BABA and Hao ZHANG

Synopsis

Due to impact of climate change, flood and sediment disasters caused by Glacial Lake Outburst Flood (GLOF) are frequently occurred in the Himalaya of South Asia or glacier regions of the world. GLOF poses a serious threat of flood disasters at downstream valley. Outburst of glacial lakes typically occurs due to moraine dam failure caused by glacier mass movement leading to a rapid rise of water level, seepage flow and a surge. The outburst of glacial lake due to moraine dam failure has been investigated. The moraine dam failure by seepage flow and overtopping due to water level rising has been investigated though a series of flume experiments. Numerical analysis of seepage and moraine dam failure has been also performed. The simulated results are compared with the experimental results. The impact of global climate change on glacial lakes is also analyzed. The empirical relationship to predict GLOF discharge has been also developed based on the recorded GLOFs discharge.

Keywords: flood disasters, GLOF, impact of climate change, moraine dam failure, numerical analysis

1. Introduction

Rainfall is a primary cause of floods and debris flow in most parts of the world. However in the Himalaya and glacier regions having glacier feed streams, glacial lake outburst is another vital cause for floods/debris flow. A study of the International Centre for Integrated Mountain Development identified about 15, 000 glaciers and 9,000 glacial lakes in Nepal, Bhutan, India, Pakistan and China, out of which 200 glacial lakes are identified as potentially dangerous in the Himalaya (Bajracharya et al., 2007a). Impacted by global warming, flood/debris flows frequently occurred in mountainous areas due to glacier outburst floods in recent years. Climate change and retreating glaciers constitute a major hazard in the Himalayas, and in similarly glacier region of the world. The Himalayan glaciers are rapidly melting due to climate change. Melting glaciers contribute to the development of glacial lakes, which may eventually glacier outburst flood for a variety of reasons, thereby causing enormous damage to surrounding communities (Osti and Egashira, 2009).

Glacial Lake Outburst Floods (GLOFs) typically occur by lake water overflowing and eroding the moraine dam. A trigger mechanism such

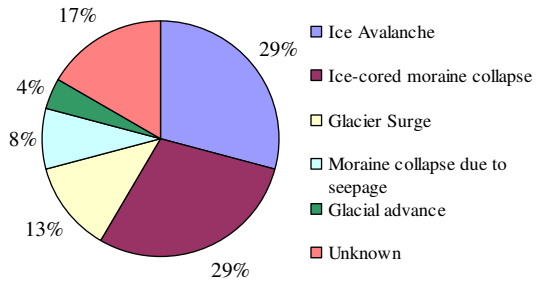

Fig. 1 Causes of 24 recorded GLOFs in the Himalaya (Data sources: Yamada (1998) and Bajracharya et al. (2006))

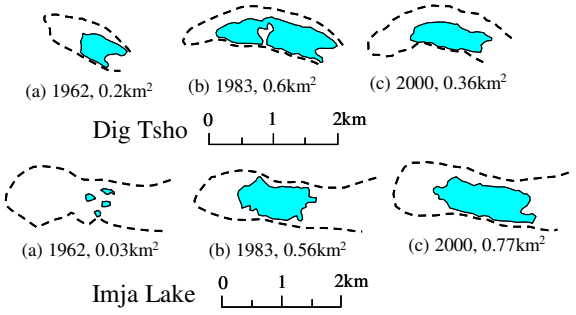

Fig. 2 Growth of Dig Tsho and Imja Glacial Lakes, Nepal (Modified from Bajracharya et al., 2007b)

Fig. 3 Satellite image of Imja Lake, Nepal (Source: Google Earth)

as displacement wave from an ice or rock avalanche, or disintegrating ice-core within the dam, or seepage/piping in the dam, or water level rising is normally required. Fig. 1 shows the causes of recorded GLOFs in the Himalaya. GLOFs pose threats of debris flow and flash floods in downstream areas (for examples, outburst flood of Ayaco glacial lake, Tibet in 1970; Zhangzangbo glacial lake, Tibet in 1981; Dig Tsho lake, Nepal in 1985; Chubung lake, Nepal in 1991; Tampokhari glacial lake, Nepal in 1998; Kabache lake, Nepal in 2003). They constituted a severe hazard to people, infrastructure and property. The studies on glacial lake outburst floods and their flood or sediment disasters in downstream areas are very limited. Therefore, there is pressing need mechanism approaches to compute the phenomenon of glacier outburst floods, downstream flooding and their preventive measures.

In this study, the outburst of glacial lake due to moraine dam failure has been investigated. The moraine dam failure by seepage flow and

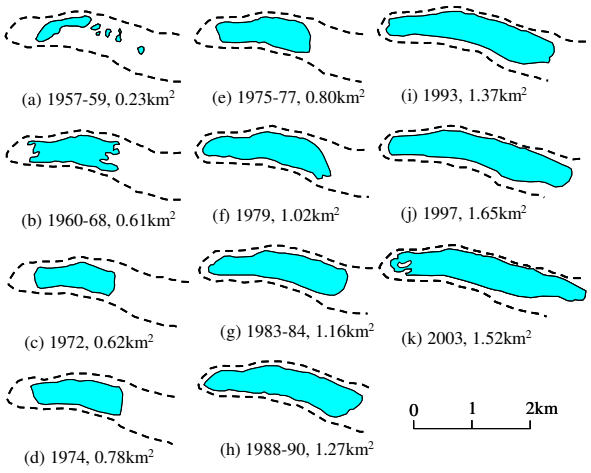

Fig. 4 Growth of Tsho Rolpa Glacial Lake in Rolwaling valley, Nepal (Modified from Horstmann, 2004)

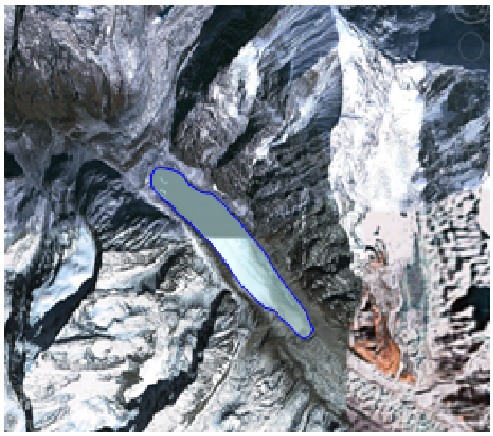

Fig. 5 Satellite image of Tsho Rolpa Lake, Nepal (Source: Google Earth)

overtopping due to water level rising has been investigated though a series of flume experiments. Numerical analyses of seepage and moraine dam failure have been also performed. The impact of global climate change on GLOF events is also analyzed. The empirical relationship to predict GLOF discharge has been also developed based on the some recorded GLOF discharge.

2. Impact of Climate Change on Glacial Lake

Glacial lakes form due to glacial melt or retreat caused by global climate change. Global warming has accelerated glacial retreat, which results the formation or expansion of glacial lakes and constitutes a major hazards in the Himalaya. The

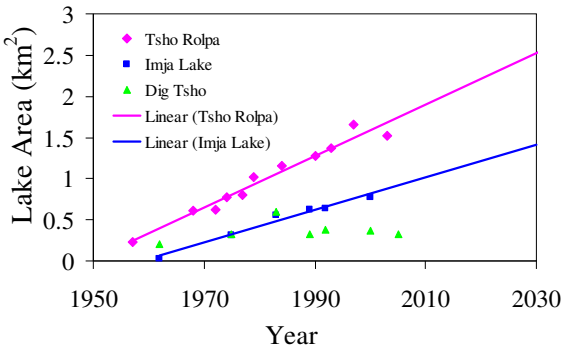

Fig. 6 Trend of lake area expansion of some glacial lakes of Nepal

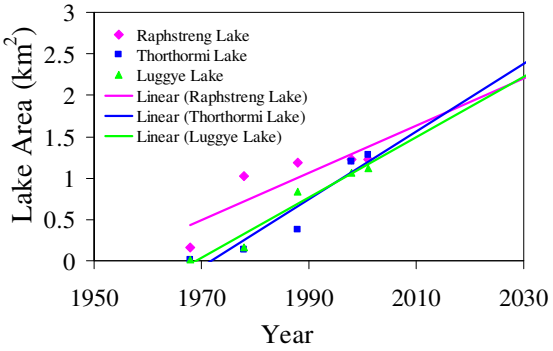

Fig. 7 Trend of lake area expansion of some glacial lakes of Bhutan

warming in the Himalayas in last three decades has been between 0.15˚C-0.6˚C per decade. Fig. 2 shows the growth of Dig Tsho and Imja Lakes in the Himalaya of Nepal, in which Dig Tsho Lake was outburst in 1985 when it attained the area of about 0.6km^2. After the outburst, the lake size of Dig Tsho is almost same as 0.36 km^2. The Imja Lake had an area about 0.03 km^2 in 1962 and 0.77 km^2 in 2000. Imja Lake is growing at a rate of 74m/year in length (Bajracharya et al., 2007a). Fig. 3 shows the satellite image of Imja Lake. Figs. 4 and 5 show the rapid growing of lake size and satellite image of Tsho Rolpa Lake, respectively. Fig. 6 shows the trend of expansion of lake area of Tsho Rolpa, Imja and Dig Tsho (outburst in 1985) lakes of Nepal and rapid expansion of lake area may cause the outburst of lake. Similar trends of rapid expansion of lake area of some glacial lakes of Bhutan are also shown in Fig. 7. The GLOF events may pose the catastrophic flooding or disasters in downstream areas. Thus, the prediction and countermeasures of flood and sediment disasters caused by GLOF events are very urgent.

3. Empirical Relationship of GLOF Discharge

Several GLOF events have occurred in the Himalaya region in the past and many of the GLOF remain unnoticed due to remoteness of its location (Dwivedi, 2005). Table 1 shows the measured discharge of some recorded GLOF events in the Himalaya of Nepal. From the regression analysis of measured discharge data of Table 1, we can get following relationship.

$$Q = 0.000850 * V * e^{-0.001822*d} \qquad (1)$$

where Q is the GLOF discharge in m^3/sec at d distance downstream from lake, V is the volume of lake water release in m^3 and d is the distance from lake in km. Fig. 8 shows the comparison

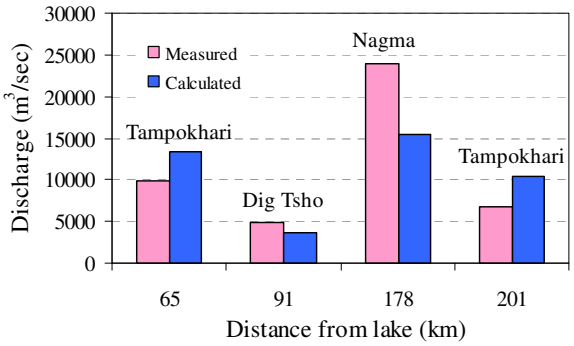

Fig. 8 Measured and calculated GLOF discharge of some glacial lakes of Nepal

Table 1 Measured GLOFs discharge

Glacial lake	Gauging station	Lake water release V (m^3)	Distance from lake d (km)	Discharge Q (m^3/sec)	Remarks
Nagma	Chatara Kothu st. 695	25,000,000	178	24,000	DHM, 2004
Dig Tsho	Rabuwa st. 670	5,000,000	91	4,800	DHM, 2004
Tampokhari	Rabuwa st. 670	17,660,000	65	9,800	DHM, 2004
Tampokhari	Chatara Kothu st. 695	17,660,000	201	6,800	DHM, 2004

Data Source: Dwivedi, 2005

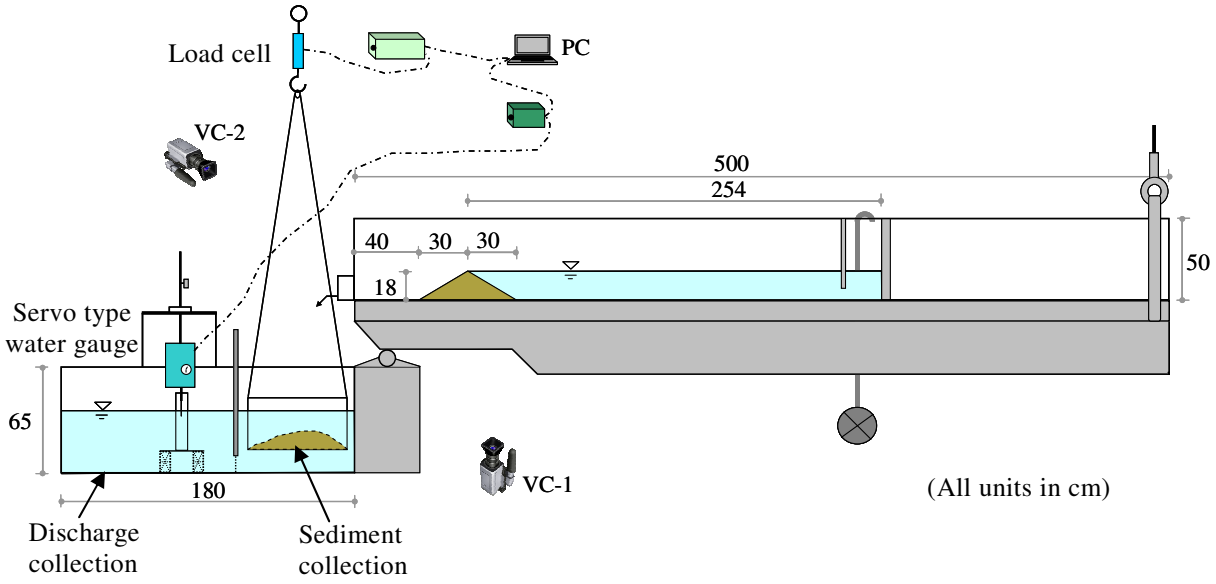

Fig. 9 Experimental flume setup

between the calculated discharge using Eq. (1) and measured GLOF discharge. Due to limited number of measured discharge and other various factors, there are some variations in the results. The maximum GLOF discharge depends on various factors such as dam characteristics, failure mechanisms, river morphology and others. So the empirical relation of maximum GLOF discharge (Eq. (1)) can be used only for rough calculation for planning infrastructures in the river.

4. Moraine Dam Failure and Outburst Discharge

4.1 Laboratory flume experiments and methods

The failure mechanism of moraine dam due to water level rising and seepage flow is investigated through the flume experiments. A 500cm long, 30cm wide and 50cm deep flume is used for the experiments. The horizontal length of upstream end of the lake reservoir from the axis of dam crest is 254cm and the length of downstream end of the flume from the axis of dam crest is 70cm as shown in Fig. 9. A dam body is made by silica sand (Sediment mix 1-6 and Sediment mix 1-7). The sediment material of sediment mix 1-6 is prepared by mixing uniformly distributed silica sand S1, S2, S3, S4, S5 and S6 in equal proportion and sediment mix 1-7 is prepared by mixing silica sand S1, S2, S3, S4, S5, S6 and S7 in equal proportion. Fig 10 shows the particle size distribution curve of the sediment materials. The mean diameter (d_m) of sediment mixes 1-6 and 1-7 are 1.4mm and 1.04mm, respectively. The maximum particle size ($d_{\max}$) and sediment density (σ) of both sediment mixes 1-6 and 1-7 are 4.75mm and 2.65g/cm^3, respectively.

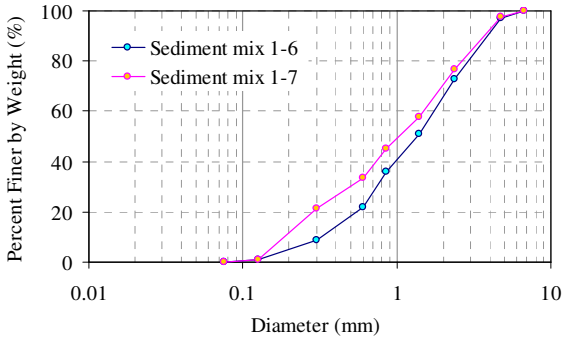

Fig. 10 Particle size distribution curve of sediment materials of the dam body

The lake water is filled by supplying a constant water discharge from the upstream end of the lake. In the case of moraine dam failure by overtopping due to water level rising, the constant water discharge is supplied continuously from upstream end of the lake to overtop the dam and erode it. However, in the case of moraine dam failure by seepage, the lake water is filled up to about 16cm in depth by supplying constant water discharge from the upstream end of the lake. Table 2 shows the

Table 2 Experimental conditions

S.N.	Case	Supply discharge Q (cm^3/sec)	Discharge supply time (sec)	Sediment mixture	Dam shape	Failure mode	Initial moisture of dam (%)	Remarks
1	Case-I	975	230	Mix 1-6	Trianguler-1	Overtopping	0.21	Exp.2
2	Case-II	975	230	Mix 1-6	Trianguler-1	Overtopping	6.67	Exp.3
3	Case-III	975	230	Mix 1-6	Trianguler-1	Overtopping	5.54	Exp.6
4	Case-IV	755	255	Mix 1-6	Trianguler-1	Overtopping	0.21	Exp.7
5	Case-V	975	230	Mix 1-6	Trapezoidal	Overtopping	0.21	Exp.9
6	Case-VI*	975	230	Mix 1-6	Trianguler-1	Overtopping	0.21	Exp.24
7	Case-VII	927	128	Mix 1-6	Trianguler-2	Seepage	4.25	Exp.11
8	Case-VIII	895	128	Mix 1-7	Trianguler-2	Seepage	5.11	Exp.13

*Erosion through initially prepared channel on the left side of dam (width=10cm and depth=1cm).

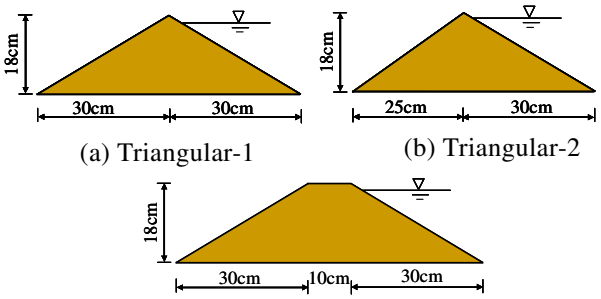

(a) Triangular-1 (b) Triangular-2

(c) Trapezoidal

Fig. 11 Details of different types of dam body

detail of the experimental conditions. The details of the dam body are shown in Fig. 11.

The outflow discharge and sediment discharge are calculated by using servo type water gauge and load cell, respectively. The temporal variations of the shapes of dam body due to erosion are captured by two video cameras located at the side and the top of the flume.

To measure the moisture movement in the dam body, the experimental cases shown in Table 2 are repeated with similar conditions. The moisture movement in the dam body is measured by using the Water Content Reflectometers (WCRs).

4.2 Experimental results and discussions

(1) Moraine dam failure by water overtopping

To investigate the moraine dam failure by overtopping and seepage, a series of flume experiments are carried out with different hydraulic conditions. Fig. 12 shows the outburst discharge at the downstream end of the flume due to moraine

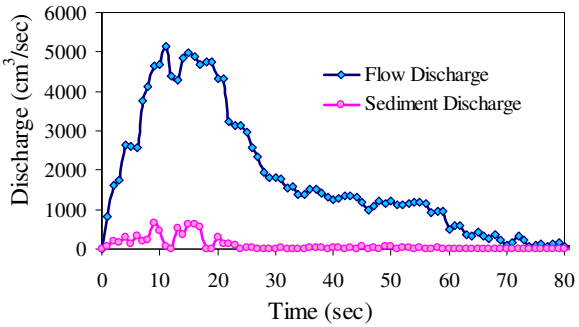

Fig. 12 Outburst discharge due to moraine dam failure by overtopping, Case-I, dry sediment case, Initial moisture content of the dam=0.21%

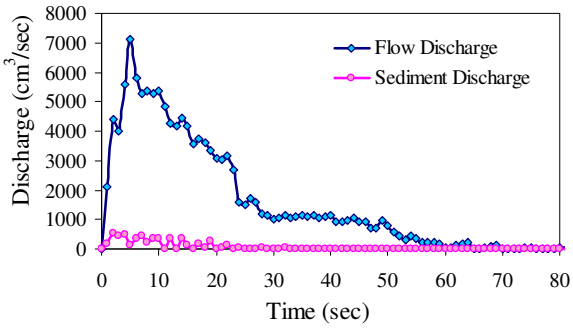

(a) Case-II, Initial moisture content of dam=6.67%

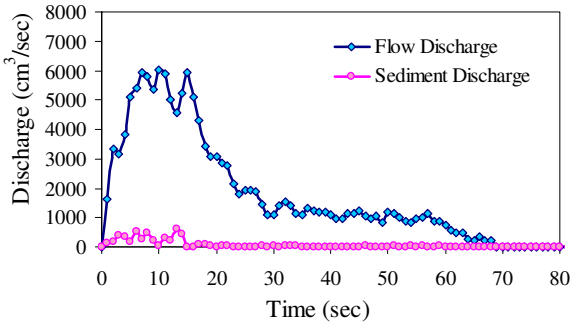

(b) Case-III, Initial moisture content of dam=5.54%

Fig. 13 Outburst discharge due to moraine dam failure by overtopping with initially some various moisture content in the dam

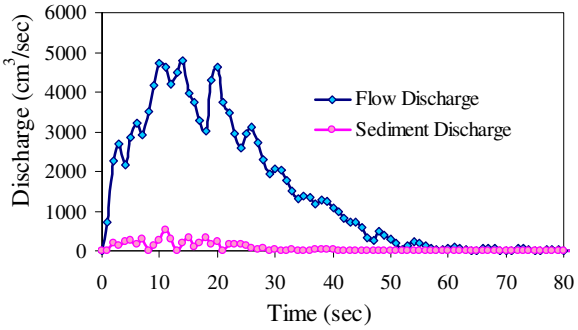

Fig. 14 Outburst discharge due to moraine dam failure by overtopping, Case-IV, Initial moisture content of dam=0.21%

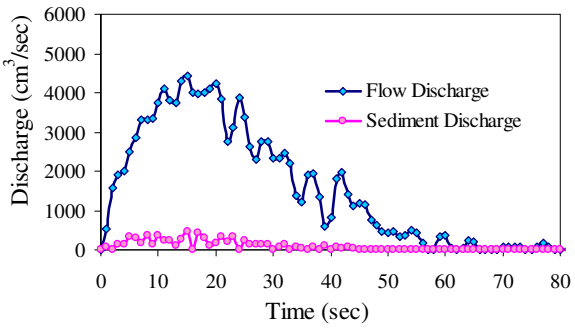

Fig. 15 Outburst discharge due to moraine dam failure by overtopping, Case-V, Initial moisture content of dam=0.21%, Trapezoidal shape of dam

dam failure by water overtopping in the experiments (Case-I). The constant discharge 975cm^3/sec is supplied from the upstream end of lake area as shown in Fig. 9. In this case, the initial moisture content of dam body is about 0.21%. Fig. 13 shows the outburst discharge due to moraine dam failure by overtopping with various initial moisture content of dam body. By comparing the results of Figs. 12 and 13 it is shown that the peak discharge is higher in the cases of 6.67% and 5.54% initial moisture content of dam than the case of 0.21% initial moisture content, which may be due to higher rate of breaching or erosion of dam with increase in moisture content. The peak discharge is increased with increase in initial moisture content of the dam body. The sediment discharge is very low with compared to the total flow discharge because the sediment volume of dam body is very smaller than volume of the lake water released (i.e., sediment volume of dam is about 1/8th of volume of lake water). The sediment concentration in the flow is due to erosion of dam surface only. However in the actual field case, the sudden release of outburst discharge from the glacial lake can rapidly erode the bed and bank along the downstream valley and poses threats of debris flows and flash floods in downstream areas.

The similar experimental results of outburst discharge due to moraine dam failure by overtopping for Case-IV and Case-V are shown in Figs. 14 and 15, respectively. By comparing the results of Figs. 12, 14 and 15 it is clear that the peak discharge of outburst is higher in the case of triangular shape of dam body than trapezoidal shape. Lake water is drawdown rapidly in the case of

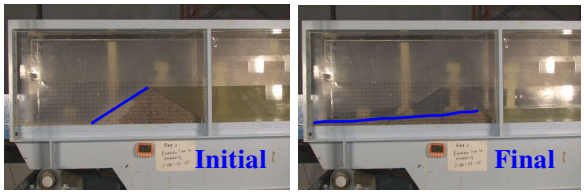

Fig. 16 Dam surface erosion in the experiment, Case-I

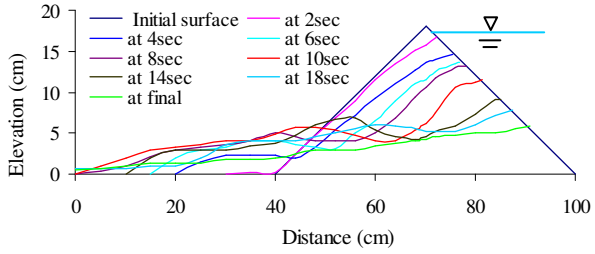

(a) Case-I, Triangular-1 shape dam

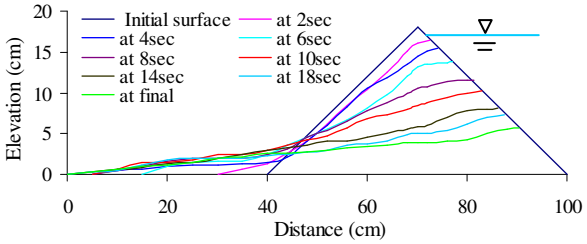

(b) Case-II, Triangular-1 shape dam

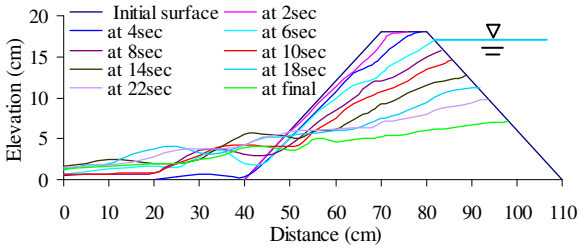

(c) Case-V, Trapezoidal shape dam

Fig. 17 Temporal variations of the shape of moraine dam due to erosion by overtopping

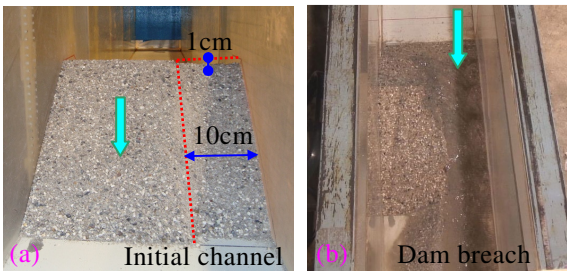

Fig. 18 (a) Partial channel on the left side of dam (width=10cm and depth=1cm) and (b) final shape of dam body due to erosion, Case-VI

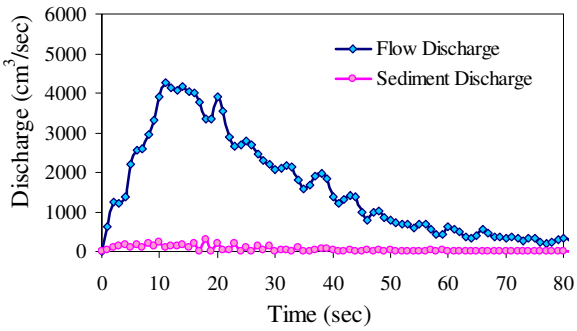

Fig. 19 Outburst discharge due to moraine dam failure by overtopping, erosion through partial channel on the left side of dam (width=10cm and depth=1cm), Case-VI

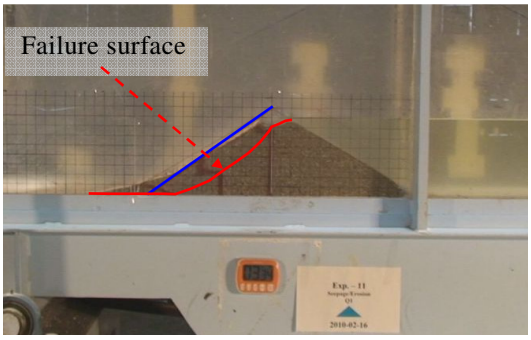

(a) Case-VII, Sediment mix 1-6

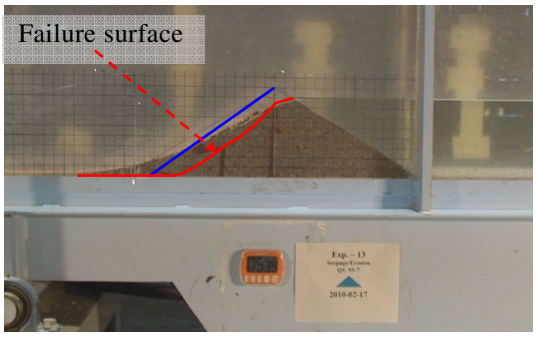

(b) Case-VIII, Sediment mix 1-7

Fig. 20 Moraine dam failure due to seepage and critical failure surface, upstream water depth is about 16cm

triangular shape of dam.

Fig. 16 shows the photographs of dam surface erosion in the experiment and Fig. 17 shows the temporal variations of the shapes of moraine dam due to erosion by lake water overtopping. After the water overtopping the crest starts to rapidly erode the dam. The triangular shape dam is eroded rapidly than trapezoidal dam body. Lake water overtopping onto the moraine dam can rapidly erode the dam and cause the failure of dam with resulting rapid drawdown of lake water. The outburst discharge from the lake may cause the catastrophic flooding in downstream areas.

The flume experiments are also carried out with breaching of dam through partial channel width. In this case, initially a channel of 10cm width and 1cm deep is made at the top surface of the dam on the left side from the crest of dam as shown in Fig. 18a. The channel starts to erode the dam by water level rising. The dam body is eroded vertically as well as laterally through the channel. However, the dam is eroded rapidly in vertical direction than lateral enlargement. The final shape of the moraine dam is shown in Fig. 18b. The outburst discharge due to moraine dam breach through partial channel width by overtopping is shown in Fig. 19.

(2) Moraine dam failure by seepage

Seepage is also one of the important trigger mechanisms for the failure of moraine dam. The flume experiments are also carried out to investigate the moraine dam failure due to seepage. The moraine dam collapse due to seepage and critical failure surface are shown in Fig. 20 for both sediment mixes 1-6 and 1-7 cases. The depth of critical failure surface is higher in the case of sediment mix 1-6 than the case of sediment mix 1-7. Thus, the depth of failure surface is strongly affected by sediment particle size. Immediately after failure of moraine dam, the lake water overtops the dam and erodes it, which results the rapid drawdown of lake water. The results of outburst discharge at the downstream end of the flume due to moraine dam failure by seepage are shown in Fig. 21 for the cases of both sediment mixes 1-6 and 1-7. The temporal variations of the

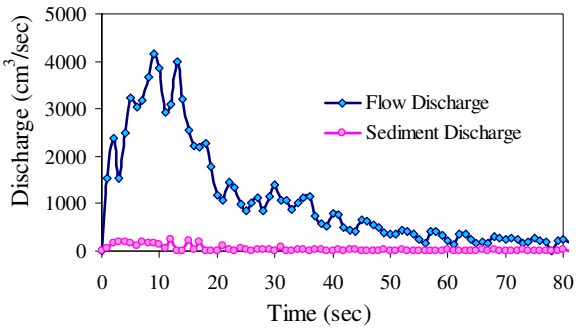

(a) Case-VII, Sediment mix 1-6

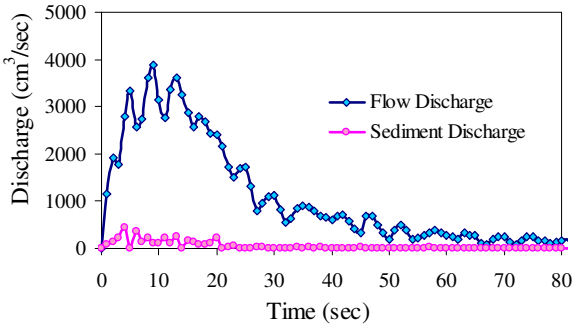

(b) Case-VIII, Sediment mix 1-7

Fig. 21 Outburst discharge due to moraine dam failure by seepage

shapes of dam due to erosion after the dam failure are shown in Fig. 22. The erosion rate of dam is smaller in the case of sediment mix with more fine sediment particles (i.e., sediment mix 1-7 case), which may be due to the effect of suction in the sediment mass of the dam.

5. Numerical Analysis of Seepage and Moraine Dam Failure

5.1 Seepage flow model

The change in pore water pressure through unsaturated-saturated soils of the moraine dam is computed by using Richards' equation as follows:

$$\frac{\partial}{\partial x}\left(K_x \frac{\partial \psi}{\partial x}\right)+\frac{\partial}{\partial z}\left(K_z\left(\frac{\partial \psi}{\partial z}+1\right)\right)=C\frac{\partial \psi}{\partial t} \qquad (2)$$

where ψ is the water pressure head, K_x and K_z are the hydraulic conductivity in x and z directions, $C\ (=\partial\theta/\partial\psi)$ is the specific moisture capacity, θ is the volumetric water content of the

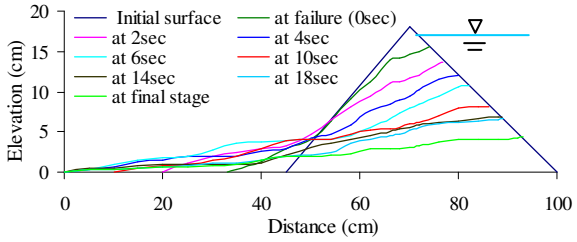

(a) Case-VII, Sediment mix 1-6

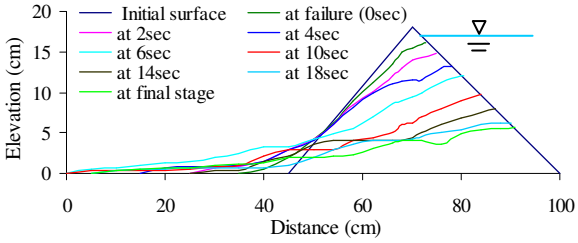

(b) Case-VIII, Sediment mix 1-7

Fig. 22 Temporal variation of the shape of moraine dam due to erosion after dam failure by seepage

soil, x is the horizontal spatial coordinate, z is the vertical spatial coordinate taken as positive upwards and t is the time.

The water storage coefficient and the coefficient of permeability are required to solve transient seepage problem associated with a unsaturated-saturated soil system using Eq. (2). Thus, the constitutive relationships given by van Genuchten (1980) are used to compute the water storage coefficient and the coefficient of permeability as follows:

$$S_e=\frac{\theta-\theta_r}{\theta_s-\theta_r}=\begin{cases}\dfrac{1}{\left(1+|\alpha\psi|^{\eta}\right)^m} & if\ \psi<0\\ 1 & if\ \psi\geq 0\end{cases} \qquad (3)$$

$$K=\begin{cases}K_s S_e^{0.5}\left[1-(1-S_e^{1/m})^m\right]^2 & if\ \psi<0\\ K_s & if\ \psi\geq 0\end{cases} \qquad (4)$$

where S_e is the effective saturation, θ_s and θ_r are saturated and residual moisture content of the sediment mix respectively, α and η are parameters related with matric potential of soil and are determined by using a curve fitting of soil-water retention curve, K_s is the saturated hydraulic conductivity and $m=1-1/\eta$. By differentiation of

Eq. (3), the relationship of the specific moisture capacity can be described as

$$C = \frac{\partial \theta}{\partial \psi} = \begin{cases} m\{1+(|\alpha\psi|)^{\eta}\}^{-m-1}\eta(|\alpha\psi|)^{\eta-1}\alpha(\theta_s-\theta_r) & if\ \psi<0 \\ 0 & if\ \psi \geq 0 \end{cases} \quad (5)$$

5.2 Slope stability model

A potential failure surface of the dam body can be computed by equating the resisting forces and driving forces applied along the failure surface. The factor of safety F_s for slip surface is defined by using the simplified Janbu's method as follows:

$$F_s = \frac{\sum R_i}{\sum T_i} \quad (i = 1, 2, 3, 4, \ldots\ldots n) \quad (6)$$

where R_i is the total normal force in each slice and T_i is the mobilized shear force in each slice. These forces can be expressed as follows:

$$R_i = \frac{cl_i\cos\alpha_i + (W_i - u_i l_i\cos\alpha_i)\tan\phi}{\cos^2\alpha_i(1+\tan\alpha_i\tan\phi/F_s)} \quad (7)$$

$$T_i = W_i\tan\alpha_i \quad (8)$$

in which c is the cohesion of the material of the dam body, l_i is the length of the base of each slice, α_i is the slope of the bottom of each slice, W_i is the weight of each slice including surface water, u_i is the average pore water pressure on the bottom of each slice and ϕ is the effective angle of internal friction.

The dynamic programming method is used to compute the critical slip surface. To minimize the factor of safety, F_s, the following subsidiary function G is defined as (Takahashi, 1991)

$$G = \sum(R_i - F_s T_i) \quad (9)$$

The minimization of factor of safety F_s is equivalent to the minimizing the function G and the minimization of function G is carried out as

$$G_m = \min G = \min\left\{\sum(R_i - F_s T_i)\right\} \quad (10)$$

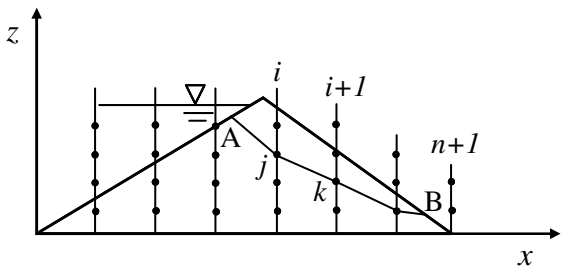

Fig. 23 Schematic figure of stages, states and critical slip surface

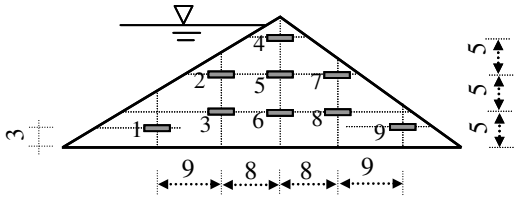

All dimensions in cm

Fig. 24 Position of 1 to 9 WCRs in the dam body

where G_m is the minimum of the function G to determine critical slip surface when F_s is less than 1.0. Initially the value of F_s is assumed and the exact value of F_s is obtained by iteration. To obtain the initial slip surface by dynamic programming method, the dam body is divided into n slices as shown in Fig. 23 and each slice boundary is divided into m_i states. An arbitrary line jk which connects points (i, j) and $(i+1, k)$ is considered as a part of assumed slip surface (Fig. 23). R_i and T_i on the surface jk are obtained from Eqs. (7) and (8) and the return function is calculated as follows:

$$DG_i(j,k) = R_i - F_s T_i \quad (11)$$

If $H_i(j)$ is the minimum value of G from the point A to the point (i, j), the minimum G value from A to $(i+1, k)$ is described as

$$H_{i+1}(k) = \min\left[H_i(j) + DG_i(j,k)\right] \quad (i = 1 \sim n, j = 1 \sim m_i, k = 1 \sim m_{i+1}) \quad (12)$$

The boundary conditions of this equation are described as

$$H_1(j) = 0, \qquad j = 1 \sim m_1 \quad (13)$$

$$G_m = \min G = \min\left[H_{n+1}(j)\right]; (j = 1 \sim m_{n+1}) \quad (14)$$

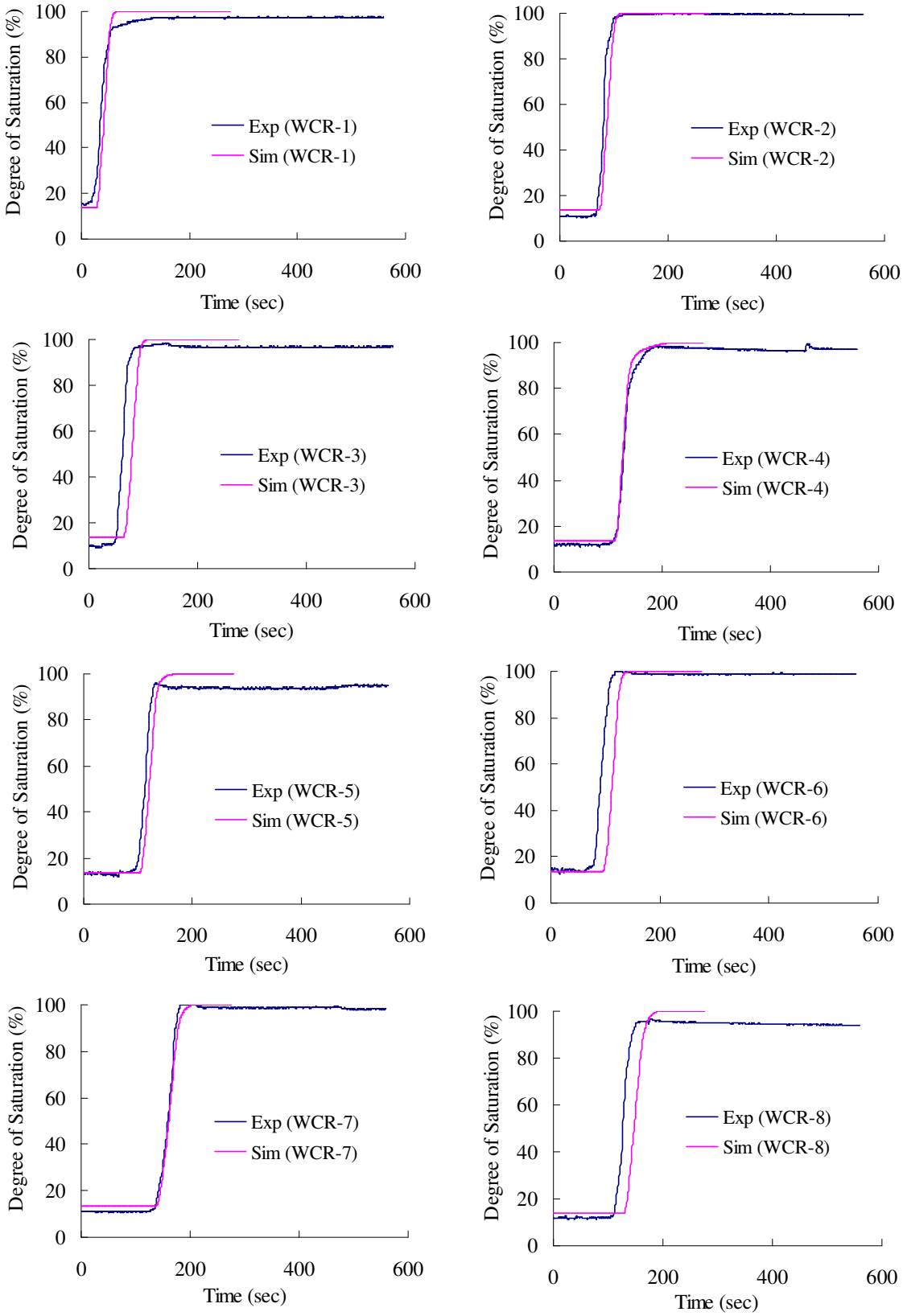

Fig. 25 Comparison of the simulated and experimental moisture content profile, Case-VII

5.3 Results and discussions

The simulated results of seepage analysis are compared with the experimental results. The moisture movement in the dam body is measured by using 9 WCRs in different location as shown in Fig. 24. The parameters of numerical analysis are as

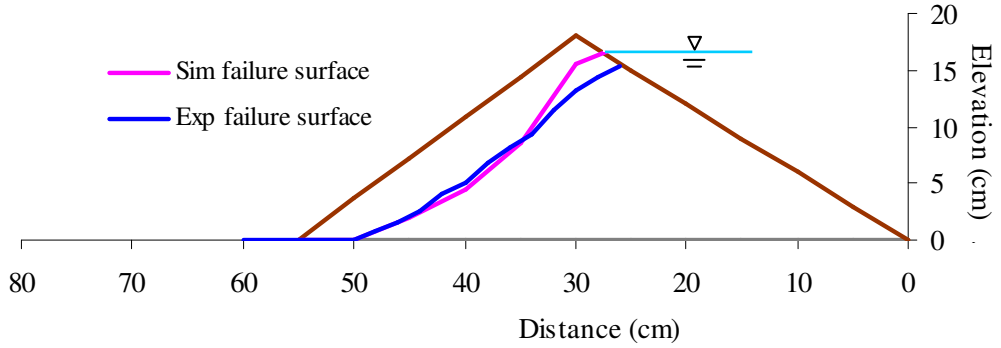

Fig. 26 Slip surface of moraine dam failure due to seepage, Sediment mix 1-6, Case VII

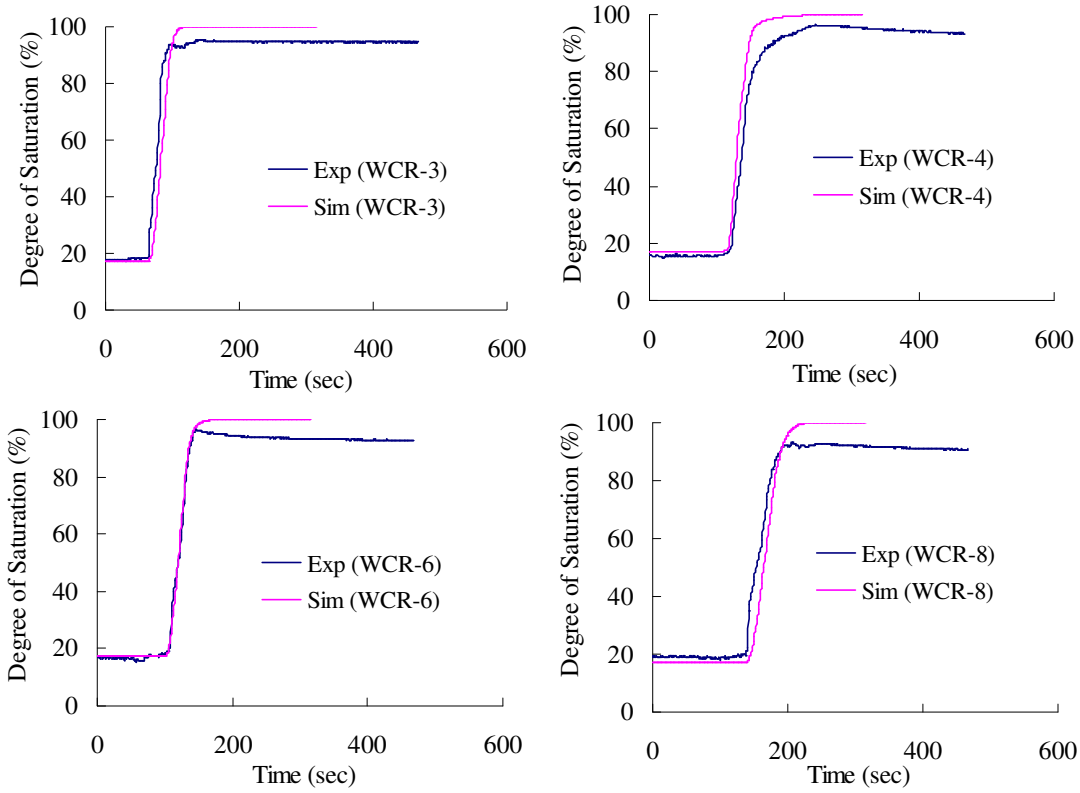

Fig. 27 Comparison of the simulated and experimental moisture content profile, Case-VIII

follows; the grid sizes $dx = 1cm$ and $dz = 0.5cm$, time interval $dt = 0.004\,\text{sec}$, the measured saturated hydraulic conductivity and saturated moisture content $K_s = 0.00055m/\text{sec}$ and $\theta_s = 0.312$ for sediment mix 1-6 and $K_s = 0.0003m/\text{sec}$ and $\theta_s = 0.296$ for sediment mix 1-7. The values of soil parameters of van Genuchten relations for sediment mix 1-6 ($\alpha = 9.6$, $\eta = 2.74$) and for sediment mix 1-7 ($\alpha = 5.5$, $\eta = 3.2$) are used as Awal (2008). The equations of seepage flow model are solved by Line Successive Over Relaxation (LSOR) scheme with an implicit iterative finite difference schemes as used by Freeze (1971, 1978). The simulated and experimental results of moisture profile in the dam are shown in Fig. 25. The simulated results are agreeable with the experimental results. The moisture movement in the dam body is due to the depth of the lake water in the upstream. The relationships of water storage coefficient and the coefficient of permeability are very important to compute the moisture movement in the unsaturated region. The moisture movement in the earth soil strongly depends on the saturated hydraulic conductivity.

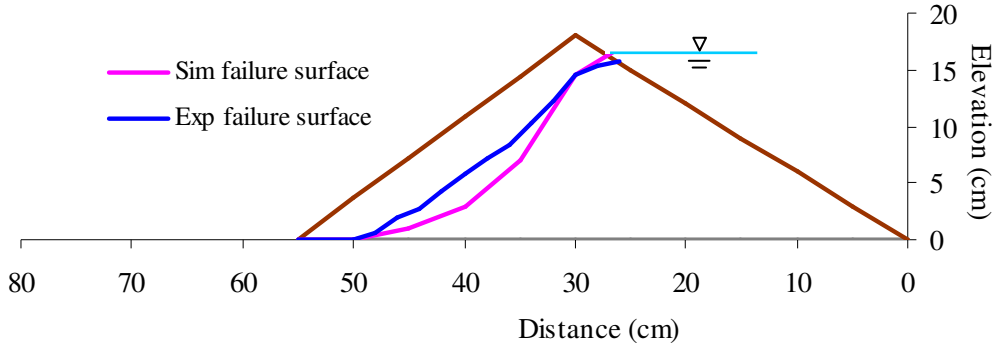

Fig. 28 Slip surface of moraine dam failure due to seepage, Sediment mix 1-7, Case VIII

Fig. 26 shows the comparison of the simulated and experimental slip surface of moraine dam failure due to seepage. In the downstream part of the dam simulated result of slip surface is very good agreement with the experimental result. However in the upstream part of the dam, there is some variation in the simulated result with compared to the experimental result, which may be due to the effect of suction in the soil strength that is not considered in the slope stability analysis and other factors. In overall, the simulated slip surface of the moraine dam failure is fairly agreeable with the experimental slip surface.

The results of moisture profile and critical failure surface with sediment mix 1-7 (Case VIII) are shown in Figs. 27 and 28, respectively. The simulated results of moisture profile are agreeable with the experimental results in this case too. However there is some variation between simulated and experimental failure surface, which may be due to the effect suction stress in the soil mass. Thus, it is also necessary to improve the slope stability model by considering suction and other factors.

6. Conclusions

The warming in the Himalayas in last three decades has been between 0.15˚C-0.6˚C per decade. The area of glacial lakes in the Himalaya is rapidly increasing in trend due to impact of global climate change, which may cause outburst of glacial lake. Hazards/disasters due to GLOF are likely to increase in intensity with the impacts of climate change. The analysis of GLOF problem in the mountainous regions of the world due to global climate change is very urgent.

The moraine dam failure due to seepage flow and water level rising are investigated through a series of flume experiments. Lake water overtopping onto the moraine dam can rapidly erode the dam and cause the failure of dam. The result of the moraine dam failure is catastrophic downstream flooding. From the analyses of experimental results, it is found that the peak discharge in the case of triangular shape dam body is higher than trapezoidal shape case. The rapid drawdown of lake water is also faster in triangular shape dam than trapezoidal shape. The empirical relation of GLOF discharge is also developed based on the observed GLOFs discharge, which can be useful for rough calculation for planning infrastructures in the river.

The numerical analyses of seepage and failure of moraine dam are also carried out and the simulated results are agreeable with the experimental results. The moisture movement in the dam body strongly effects on the stability of the dam by decreasing the shear strength of the sediment mixture of the dam body.

An integrated numerical model has been also developing to simulate the outburst discharge of glacial lake due to moraine dam failure by seepage and overtopping. In future research, the characteristics of flood disasters and hazardous zone caused by outburst of most potential dangerous glacial lakes Imja and Tsho Rolpa of Nepal will be prepared by using numerical model

and Geographical Information System (GIS) tools with various scenarios.

Acknowledgements

The authors are grateful to the GCOE program 'Sustainability/Survivability Science for a Resilient Society Adaptable to Extreme Weather Conditions' of Disaster Prevention Research Institute, Kyoto University for providing financial support for this research work and also for providing Young Scientist Research Grant to the first author. The authors are also wish to thank Mr. Satoshi Kohda for his help in translation of English synopsis into Japanese.

References

Awal, R. (2008): Study on landslide dam failure due to sliding and overtopping, Doctoral Thesis, Kyoto University.

Bajracharya, S. R., Mool, P. K., and Shrestha, B. R. (2006): The impact of global warming on the glaciers of the Himalaya, International Symposium on Geo-disasters, Infrastructure Management and Protection of World Heritage Sites, Nepal Engineering College, Ehime University and National Society for Earthquake Technology Nepal, pp.231-242.

Bajracharya, S. R., Mool, P. K., and Shrestha, B. R. (2007a): Impact of climate change on Himalayan glaciers and glacial lakes, case studies on GLOF and associated hazards in Nepal and Bhutan, ICIMOD and UNEP, pp.1-119.

Bajracharya, B., Shrestha, A. B. and Rajbhandari, L. (2007b): Glacial lake outburst floods in the Sagarmatha region, Mountain Research and Development, Vol. 27, No. 4, pp.336-344.

Dwivedi, S. K. (2005): Downstream impacts of glacier lake outburst flood in the Himalaya, Proceedings of International Conference on Monitoring, Prediction and Mitigation of Water-Related Disasters (MPMD-2005), Disaster Prevention Research Institute, Kyoto University, pp.387-393.

Freeze, R. A. (1971): Influence of the unsaturated flow domain on seepage through earth dams, Water Resources Research, Vol. 7, pp.929-941.

Freeze, R. A. (1978): Mathematical models of hillslope hydrology, In M. J. Kirkby, (ed), Hillslope Hydrology, John Wiley, pp.177-225.

Horstmann, B. (2004): Glacial lake outburst floods in Nepal and Switzerland－new threats due to climate change, Germanwatch, pp.1-11. http://www.germanwatch.org/download/klak/fb-gl-e.pdf (accessed 26 April 2010).

Osti, R. and Egashira, S. (2009): Hydrodynamic characteristics of the Tam Pokhari glacial lake outburst flood in the Mt. Everest region, Nepal, Hydrological Processes, Vol. 23, pp.2943–2955.

Takahashi, T. (1991): Debris flow, Monograph Series of IAHR, Balkema.

van Genuchten, M. T. (1980): A closed-form equation for predicting the hydraulic conductivity of unsaturated soils, Soil Science Society of America Journal, Vol. 44, pp.892-898.

Yamada, T. (1998): Glacier lake and its outburst flood in the Nepal Himalaya, Data Center for Glacier Research, Japanese Society of Snow and Ice, Monograph No. 1, pp.1-96.

気候変動に伴う浸透と越流によるモレーンダム破壊に起因する氷河湖の決壊

Badri Bhakta SHRESTHA・中川一・川池健司・馬場康之・張浩

要　旨

気候変動に起因する氷河湖決壊洪水（GLOF）による洪水災害と土砂災害は南アジアのヒマラヤ地域やその他の氷河地帯においてたびたび発生し，下流において深刻な洪水災害をもたらす脅威となっている。氷河湖の決壊の主な原因は，氷塊の移動が急激な水位上昇や浸透流，氷河サージを引き起こし，それによってモレーンダムが破壊されることである。本報は，モレーンダムの破壊に起因する氷河湖決壊を研究したものである。浸透流と水位上昇による越流がもたらすモレーンダム破壊を一連の実験によって検証し，浸透とモレーンダムの破壊について行った数値解析結果と比較した。また，氷河湖に与える全球気候変化の影響も解析し，観測記録にもとづいて氷河湖決壊洪水流量を予測する経験的関係を導いた。

キーワード：洪水災害，氷河湖決壊洪水，気候変動，モレーンダム決壊，数値解析